9th Asia-Pacific Conference on Wind Engineering
Auckland, New Zealand
3-7 December 2017

Experimental Study on Aerodynamic Characteristics of Rectangular Cylinder with Appendages for Various Angle of Attack

S. Nakato[1]

[1]Department of Science and Engineering
Kanto-gakuin University, Yokohama, Japan

Abstract

The objective of this study is to investigate aerodynamic characteristics for cylinder with cross section of square and others using wind tunnel testing. Experimental procedure employing a load cell with one direction, rotary actuator and so on is confirmed by good agreement with existing data for square cylinder case. Fluctuating lift coefficient can be evaluated properly by summation over 1/3 octave band around peak from power spectra without band pass filter in measuring. Appendages, which is inhomogeneous along longitudinal direction of model, is effective for suppress the peak and correlation in some range of angle of attack.

Introduction

Aerodynamic characteristics of rectangular cylinder are of considerable interest in wind engineering, as well as that of circular cylinder. A number of investigations were carried out by many researchers [1]. Dependence on Reynolds number is major concerned on circular cylinder. On the other hand, dependence of side ratio and angle of attack is major concerned on rectangular cylinder, but in past study these data is not enough, especially for fluctuating value like fluctuating drag and lift coefficient, correlation length, power spectrum and so on.

Unstable aerodynamic phenomena around cylinder-like structure such as bridge, building, transmission wire, etc. caused vortex-induced vibration (VIV), galloping and flutter. Flow induced vibration is major engineering issue. From point of view of structural mechanism, a fundamental solution is strengthening structure. Actually, for instance, concrete structure of short span bridges or low building do not have wind-causing problem. From point of view of fluid mechanism, suppression of fluctuating aerodynamic force is required. Modification of cross section shape is also effective, and, for example, corner cutting is one of the aerodynamic stabilization methods. Spiral strand is also implemented to cable of suspension bridges.

The author studied aerodynamic characteristics of rectangular cylinder with respect to wind speed [2]. The objective of this study is to clarify the frequency-domain characteristics for cylinder with cross section of square and others, especially concerning angle of attack. In addition, feature of inhomogeneous cross section along longitudinal axis is also investigated.

Experimental setup

The Eiffel type wind tunnel was used in this study. The size of test section is 0.4 m ×0.4 m. The maximum wind velocity is 11.1 m/s and turbulence intensity is 1 %. The experimental results at 8.4 m/s are mainly shown here.

The aerodynamic forces are measured by using load cell where the cylinder model rigidly supported as cantilever beam. The sampling rate is 2000Hz with sampling time of 10 sec. In typical case of this experiment, peak frequency is about 100 Hz and 1000 waves is contained in a measurement data, which is considered enough for precise frequency resolution. Load cell has two screw holes having M4 of nominal size with centre distance of 10mm. The model was fixed by two screws. A load cell is connected to a strain amplifier (DPM-712B, Kyowa Co. Ltd) with a range of 100 με and 1kHz low-pass filter. The position of the model and the sensor is moved easily for flexibility of experimental condition and settled by a laser-marking device. Its accuracy is lower than traverse apparatus settled to wind tunnel.

Two-hot wires with distance of 45mm (3d) is located at x=45mm along wind direction, z=30mm along vertical direction, where origin is centre of model. These fluctuating velocities are used not only for coherence in the wake but also detecting peak frequency of vortex shedding.

Changing angle of attack with small increment

Smoothness of measurement data is one of effective indicators to evaluate reliability of measurement. For instance, when flow pattern around cylinder with sharp edges like square cylinder does not change with increment of wind speed, Strouhal number and drag coefficient give constant value. So if these values are not constant, usually this is caused by not physical mechanism but experimental condition. In case of circular cylinder, its Strouhal number and drag coefficient depend on wind speed (Reynolds number) and if increment of wind seed is small enough, their change is supposed to be smooth. In addition, you can find drag crisis at around Re=1.0×10^5 by increasing wind speed little by little. Similar things occur for square cylinder. If angle of attack is increased, Strouhal number shows sharp peak at angle of attack 12-13°. This sharp peak is overlooked with large increment.

Changing condition with small increment of angle of attack, wind speed, dimension of model, etc. is useful to evaluate scattering values related to fluctuating phenomena. Recording long time data is also important for stationary data. One more way is gathering many data in different experimental apparatus. In this study, angle of attack is changed by small increment, employing rotary actuator (DGM85R-ARAC, Oriental motor. co. ltd.) with minimum step of 0.02°. End of the load cell, which is opposite side to model-fixed end, is fixed to rotary actuator. In this experiment, angle of attack is increased by 1°.

Models

Models shown in Figure 1 are beam-like structure as follows; a) square cylinder of 15 mm on side, b) square cylinder with appendages of 5mm height, 20mm width and 15mm length with each gap of 10 mm, c) girder-like model, having plate of 3 mm height and 30 mm width on the square cylinder and d) girder-like model with appendages of 10mm height, 30mm width and 5 mm thickness with each gap of 20 mm. Aspect ratio L/D=26.7 for all models. Square cylinder of a) and b) is made of aluminium pipe, and others are made of wood.

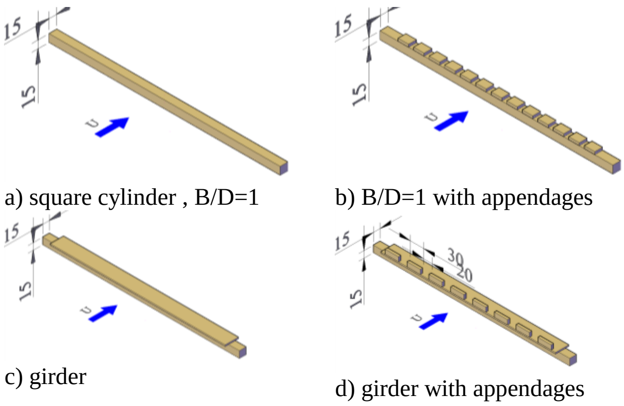

Figure 1 Models

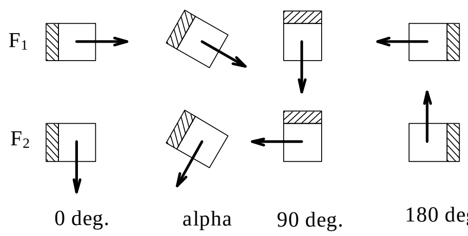

Figure 3 Arrangement of models with direction of force measured by load cell, the case of model b)

Data analysis

Spectral analysis is applied to fluctuating force and fluctuating velocity in the wake. Peak frequency related to dominant periodic components is obtained from spectrum of fluctuating velocity because fluctuating force may have another peak related to structural components. From spectra of fluctuating force, peak value in a range of 1/3 octave band is obtained as well as ordinary peak value. As frequency resolution is 1 Hz in this study, if f_{peak}=100Hz, the range of $f_{1/3}$ octave is from 79 to 126 Hz. Furthermore correlation index β is defined as follows;

$$\beta = P(f_{peak})/P(f_{1/3oct.}) \quad \cdots\cdots (1)$$

When β=1, peak is very sharp which means time history is pure sinusoidal. While when β<<1, peak is not significant which means time history is noisy.

Results and discussion

Square cylinder B/D=1 with/without Appendages

Figure 2 shows time histories for coefficients of lift force with wind speed of 8.4 m/s. Lift force, mainly caused by vortex shedding, is not purely sinusoidal even for square cylinder due to long aspect ratio. For square cylinder with appendages, disturbance increases.

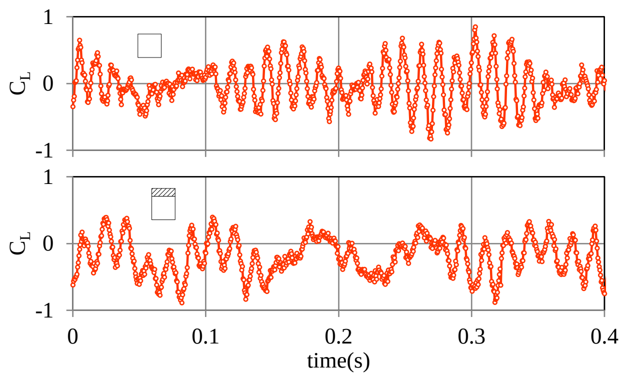

Figure 2 Time histories for coefficients of lift, top: model a), bottom: model b), angle of attack=0°

Load cell with one direction is used in this experiment, therefore two measurement series are carried out for one model as shown in Figure 3. Drag and lift are calculated as follows at arbitrary angle of attack α;

$$D(\alpha) = F_1(\alpha)\cdot\cos\alpha - F_2(\alpha)\cdot\sin\alpha$$
$$L(\alpha) = -F_1(\alpha)\cdot\sin\alpha - F_2(\alpha)\cdot\cos\alpha \quad \cdots\cdots (2)$$

Drag and lift coefficients for B/D=1, square prism, are shown in Figure 4. Drag coefficient degreases gradually, reached a dip at α=12° where reattachment of separated flow occurs. After that, it increases gradually. Drag coefficient at 0° is 2.23, which is corresponding to existing data. The obtained C_D and C_L are in good agreement with past results in literature [3] (obtained from surface pressure data). For mean value, measurement data from load cell with one direction is enough for obtaining stable data.

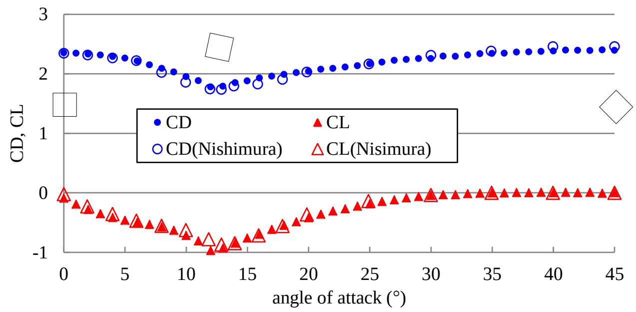

Figure 4 Drag and lift coefficients, B/D=1: comparison with results in literature

In Figure 5, drag and lift coefficients of B/D=1 with appendages show same tendency with B/D=1 in sense of having peak or dip at angle of attack where separated flow is reattaching. It is distinctive that peak is milder than that of B/D=1 at around 8° and 75° where edge of appendages faces windward. At 0, 90 , and 180°, lift supposed to be zero because cross section is symmetry vertically, but result is not zero at 0, 180°. In this experiment, first output of the load cell was measured with windless condition, by which measurement value in wind was subtracted. Model supporting condition or sensor condition might be changed between these measurements.

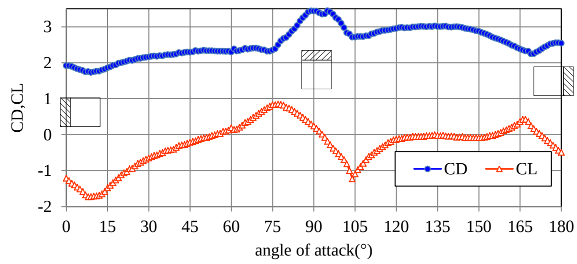

Figure 5 Drag and lift coefficients, B/D=1 with appendages

Power spectral density of force obtained from the load cell directly (eq. (2) is not applied), whose axis is perpendicular to horizontal axis of model, is shown in Figure 6. An arrow in cross section means direction of the measured load. Each plot at angle of attack from 70 to 110 deg. is placed along downward direction with shift of 10dB. Note that 2 or 3 peaks in the low frequency range, probably resulting from natural frequency of structure, exist due to not using bandpass filter in measuring. Natural frequency of model is 13 Hz by free vibration test, which is corresponding to the lowest frequency peak in spectra. For

B/D=1 with appendages, peak frequency changes slightly comparing with B/D=1.

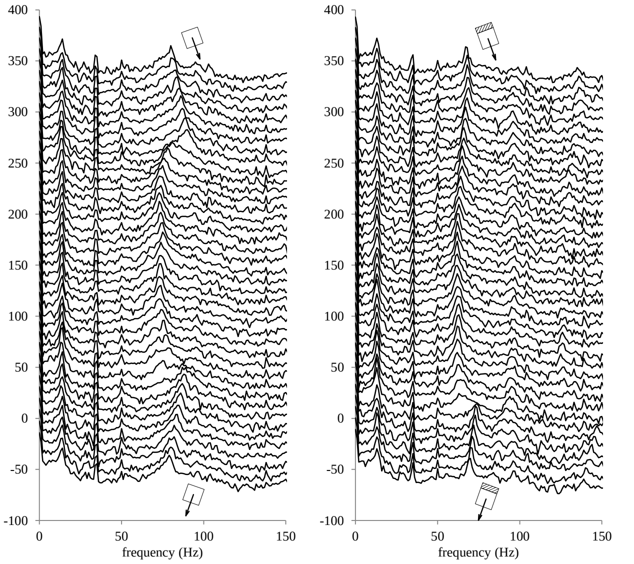

Figure 6 Power spectral density of aerodynamic force, α=70~110°, left: B/D=1, right: B/D=1 with appendages. The 10 dB shift between successive cases.

Strouhal number obtained from peak of power spectra of fluctuating velocity in the wake is shown in Figure 7. Strouhal number is defined as follows;

$$St = f_p D / U \quad (3)$$

where f_p is peak frequency, D is representative length (D=15mm), and U is wind speed. Present St number is good agreement with existing data [3] and has peak at around 13°. It can be also observed that there is dip at around 5° in present data.

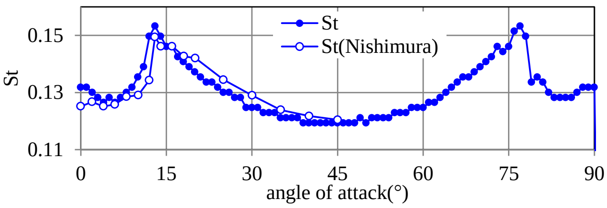

Figure 7 Strouhal number and angle of attack

Fluctuating drag and fluctuating lift coefficients, induced by three methods, are shown in Figure 8. Filled markers mean peak value per 1 Hz, while outline markers means peak value per 1/3 octave band where centre is peak frequency. They have same tendency for C_D' and C_L' respectively, but magnitude of 1/3 octave peak is about three times larger than 1 Hz peak. Value of C_L' increases gradually as the angle increases and reaches constant value at high angle. Value of C_L' has peak at 3 degree as well as 0 degree, in other ward, there is dip 1 or 3 degree. Outline markers with dotted line is ordinary definition of RMS value, but it is not useful because it is affected by low frequency peak as shown in Figure 6.

Present results of 1/3 octave peak have same tendency with existing data [3] shown in bottom plot of Figure 8, but their values are one-fifth value of them. This is probably because the data in reference [3] obtained from surface pressure at one section, therefore fluctuating lift is almost sinusoidal. On the other hand, in this data, fluctuating lift is summation of all sectional lift along longitudinal axis of the cylinder model.

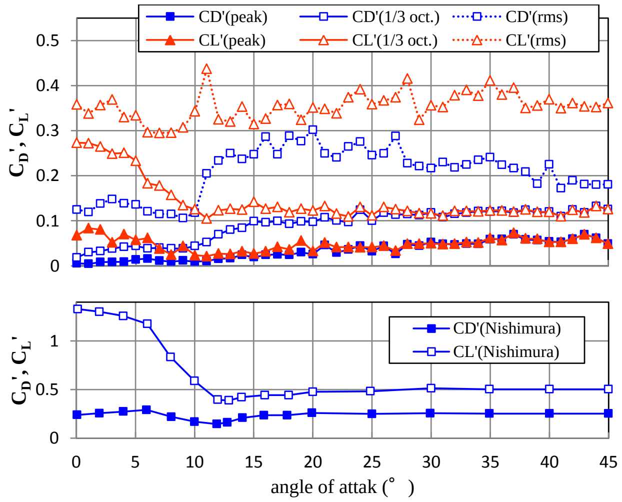

Figure 8 Coefficients of fluctuating drag and lift, B/D=1

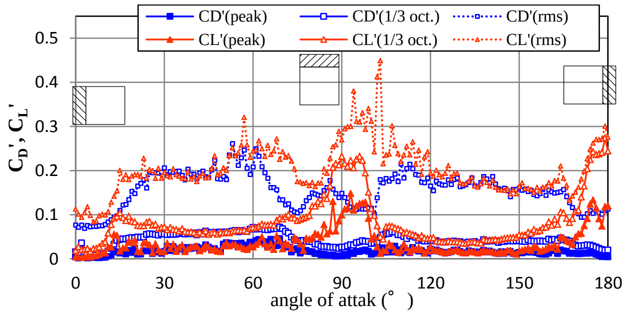

Figure 9 Coefficients of fluctuating drag and lift, B/D=1 with appendages

Coherence between two hot-wires in B/D=1 is shown in Figure 10. Although measurement value is scattering, some tendency is observed. Coherence is high at angle of around 45°and low at around 0° (90°). When hot-wire is positioned at flow-reattaching side (α=81~84°), coherence becomes small. It is noticed that the values at 0° and 90° should be same, but there is discrepancy. Coherence value is not stable in comparison with mean aerodynamic force or St number. Correlation index β induced by eq. (1) is also shown in Figure 10. Both tendencies are almost same, but spiky values do not correspond each other. When appendages are added, coherence is reduced at around 0°.

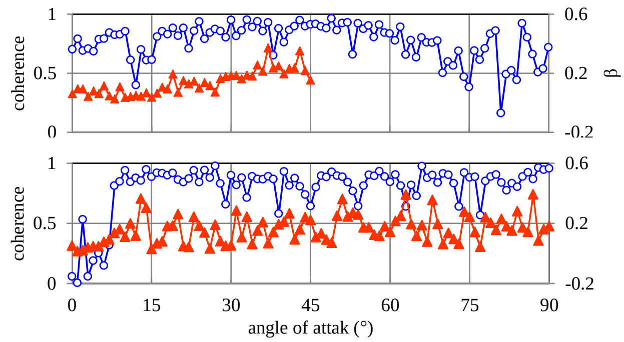

Figure 10 Coherence (○) and Correlation index β (▲)
top: B/D=1, bottom: B/D=1 with appendages

Girder with/without appendages

Drag and lift coefficients, C_D and C_L for girder without/with appendages shown in Figure 11. For girder C_L has peak at −6°, while C_D is larger in positive angle. For girder with appendages, rapid change occurs around at 0°. Comparing both C_D, that of girder with appendages is larger in positive angle because projection area increases by appendages.

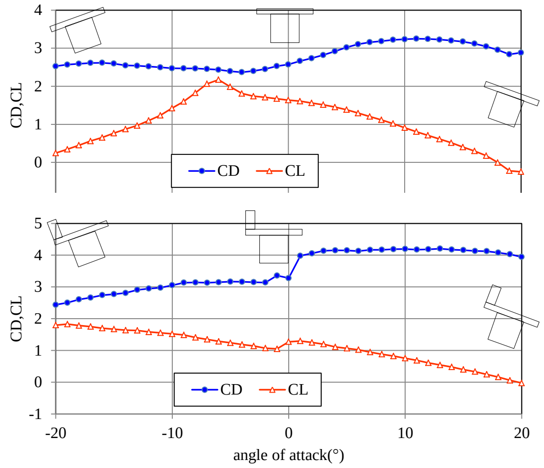

Figure 11 Drag and lift coefficients,
top: girder, bottom: girder with appendages

Power spectral density of force for the girder model without/with appendages at angle of attack from -20 to 20° is shown in Figure 12 in the same manner as Figure 6. Natural frequency of the girder model is 13 Hz obtained from free vibration test. For the girder model, frequency of peak increases monotonically as angle of attack increases to -6°, corresponding to maximum of lift in Figure 11. After this angle, frequency of peak is almost constant. For the girder with appendages, such peak disappears in negative angle of attack. This is caused by jet-like flow through the gap of appendages at front of the model. In positive angle of attack, peak appears.

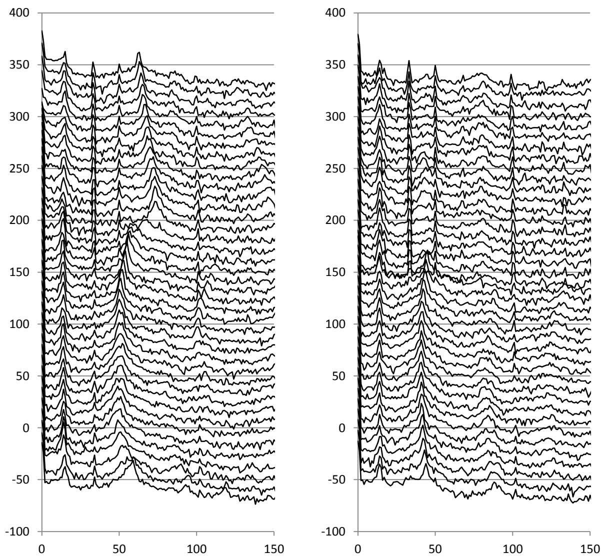

Figure 12 Power spectra of load, left: girder, right: girder with appendages

Coefficients of fluctuating drag and lift for girder and girder with appendages are shown in Figure 13. For fluctuating lift coefficient, contrasting result between negative and positive angle of attack is obtained because peak value is smaller in negative side.

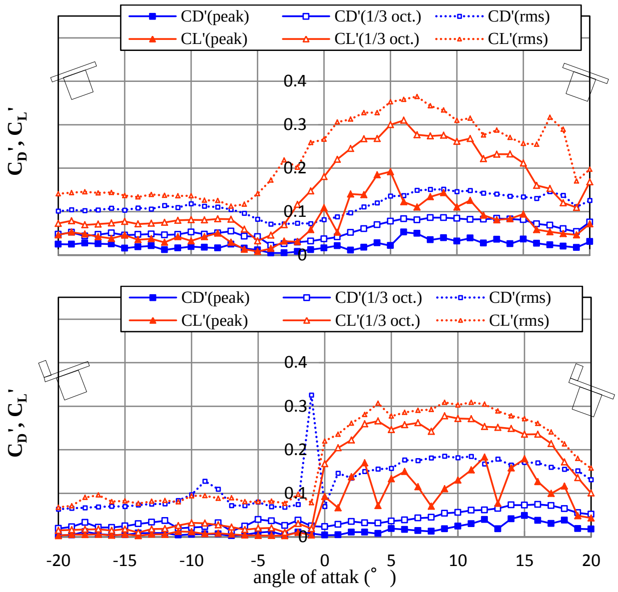

Figure 13 Coefficients of fluctuating drag and lift,
top: girder, bottom: girder with appendages

For girder, coherence and correlation index β show same tendency. For girder with appendages, coherence is scattering because fluctuating velocity is affected by jet-like flow through the gap of appendages.

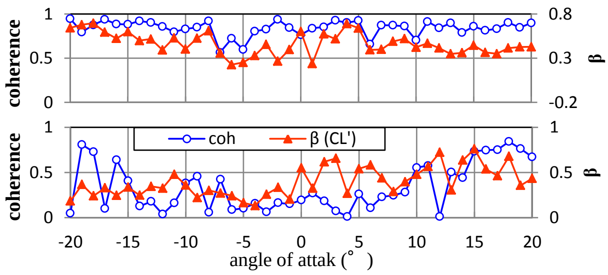

Figure 14 Coherence and Correlation index β,
top: girder, bottom: girder with appendages

Conclusions

In this paper, aerodynamic characteristics of square cylinder and girder-like cylinder with/without inhomogeneous appendages along longitudinal direction were investigated. Effect of appendages is observed in shifting peak frequency, suppressing peak and reducing spanwise correlation in some angle of attack. It is future work to improve the experimental condition for obtaining more accurate quantitative value.

References

[1] E. Naudascher, Hydrodynamic Forces, A.A. Balkema, 1991.

[2] S. Nakato, "Spatial Correlation of Fluctuating Lift for 2D Cylinder and Cylinder with Different Cross Sections," *Proceedings of the 24th National Symposium on Wind Engineering*, pp. 193-198, 2016, (in Japanese).

[3] H. Nishimura and Y. Taniike, "Fluctuating Wind Forces on a Stationary Two-Dim. Square Prism," *Proceedings of the 16th National Symposium on Wind Engineering*, pp. 255-260. (in Japanese), 2000.